GEOPHYSICAL RESEARCH LETTERS, VOL. 35, L01105, doi:10.1029/2007GL032009, 2008

Discovery of very large amplitude whistler-mode waves in Earth's radiation belts

C. Cattell,[1] J. R. Wygant,[1] K. Goetz,[1] K. Kersten,[1] P. J. Kellogg,[1] T. von Rosenvinge,[2] S. D. Bale,[3,4] I. Roth,[3] M. Temerin,[3] M. K. Hudson,[5] R. A. Mewaldt,[6] M. Wiedenbeck,[7] M. Maksimovic,[8] R. Ergun,[9] M. Acuna,[2] and C. T. Russell[10]

Received 13 September 2007; revised 30 October 2007; accepted 6 December 2007; published 12 January 2008.

[1] During a passage through the Earth's dawn-side outer radiation belt, whistler-mode waves with amplitudes up to more than ~240 mV/m were observed by the STEREO S/WAVES instrument. These waves are an order of magnitude larger than previously observed for whistlers in the radiation belt. Although the peak frequency is similar to whistler chorus, there are distinct differences from chorus, in addition to the larger amplitudes, including the lack of drift in frequency and the oblique propagation with a large longitudinal electric field component. Simulations show that these large amplitude waves can energize an electron by the order of an MeV in less than 0.1s, explaining the rapid enhancement in electron intensities observed between the STEREO-B and STEREO-A passage during this event. Our results show that the usual theoretical models of electron energization and scattering via small-amplitude waves, with timescales of hours to days, may be inadequate for understanding radiation belt dynamics. **Citation:** Cattell, C., et al. (2008), Discovery of very large amplitude whistler-mode waves in Earth's radiation belts, *Geophys. Res. Lett.*, *35*, L01105, doi:10.1029/2007GL032009.

1. Introduction

[2] It has long been known that the Earth's magnetosphere is an extremely efficient accelerator of relativistic particles that make up the Van Allen radiation belts. The mechanisms via which this acceleration occurs, however, remain a source of controversy and processes occurring on a variety of timescales have been proposed [*Friedel et al.*, 2002; *Hudson et al.*, 2007]. The radiation belts consist of an inner belt at ~1.5 R_e (Earth radii) and a more dynamic outer belt peaking near ~4 R_e, both trapped on Earth's dipole magnetic field lines. Although whistler-mode electromagnetic waves have long been invoked as a mechanism for loss of electrons from the radiation belts [*Kennel and Petschek*, 1966], it is only recently that their role in electron energization has been evaluated and compared to other acceleration mechanisms such as radial diffusion [*Schulz and Lanzerotti*, 1974]. Acceleration of electrons by low amplitude whistler-mode 'chorus' waves is currently accepted to be an important process in the outer belt [*Summers et al.*, 1998; *Roth et al.*, 1999; *Summers and Ma*, 2000; *Meredith et al.*, 2001; *Horne and Thorne*, 2003; *Horne et al.*, 2005; *Albert and Young*, 2005]. Theoretical studies of both loss and acceleration mechanisms usually assume that the whistler waves are low amplitude and that acceleration occurs via multiple stochastic interactions with a large number of uncorrelated wave packets, so that the quasi-linear approach can be utilized. The assumption of small amplitudes is consistent with statistical studies of the waves [*Meredith et al.*, 2001; *Horne et al.*, 2005]. Because plasma waves in space have traditionally been observed using instruments which measure in the frequency domain and which often have time resolutions long compared to the time scales over which wave amplitudes vary, studies of existing databases may have underestimated the occurrence of large amplitude waves. This problem is intensified in studies that examined long-time or large-spatial averages or used instruments that saturate at low amplitudes. The largest whistler amplitudes reported to date (~30 mV/m) were observed by the Cluster spacecraft [*Santolík et al.*, 2003] using a wideband plasma wave instrument (WBD) designed to capture waveforms, enabling examination of rapidly varying amplitudes [*Gurnett et al.*, 1997]. However, the WBD was not designed to target large amplitude waves. It does not trigger waveform capture or data storage and transmission based on wave amplitudes and can have low saturation amplitudes. The other Cluster waveform instrument (part of EFW [*Gustaffson et al.*, 1997]) obtained only a few captures per day, primarily in the outer magnetosphere. For these reasons, very few high-resolution and/or high amplitude waveform samples have been obtained in the Van Allen belts. To understand the role of whistlers in radiation belt dynamics, it is necessary to determine how often large amplitude waves occur, the wave properties and how their effects compare to those resulting from lower amplitude whistlers analyzed in previous studies.

[1]School of Physics and Astronomy, University of Minnesota, Minneapolis, Minnesota, USA.
[2]NASA Goddard Space Flight Center, Greenbelt, Maryland, USA.
[3]Space Sciences Laboratory, University of California, Berkeley, California, USA.
[4]Department of Physics, University of California, Berkeley, California, USA.
[5]Department of Physics, Dartmouth College, Hanover, New Hampshire, USA.
[6]Downs Laboratory, California Institute of Technology, Pasadena, California, USA.
[7]Jet Propulsion Laboratory, California Institute of Technology, Pasadena, California, USA.
[8]Laboratoire d'Etudes Spatiales et d'Instrumentation en Astrophysique, Observatoire de Paris, Meudon, France.
[9]Laboratory for Atmospheric and Space Physics, University of Colorado, Boulder, Colorado, USA.
[10]Institute for Geophysics and Planetary Physics, University of California, Los Angeles, California, USA.

0094-8276/08/2007GL032009$05.00

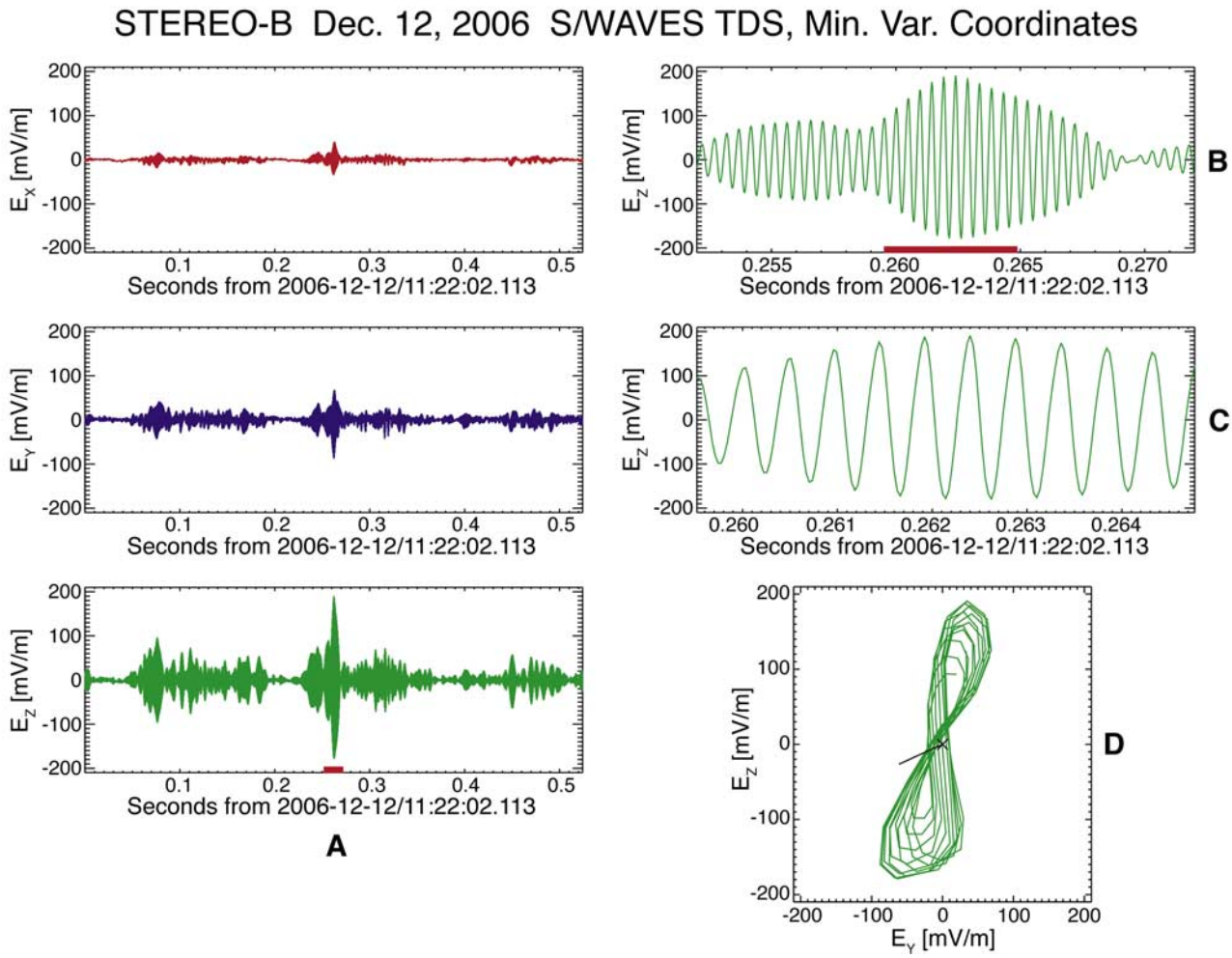

Figure 1. The whistler waveform for a representative TDS sample selected from the 24 obtained during the 4 minute interval from ∼1120–1124 UT. (a) The three components of electric field in minimum variance coordinates. (b) An expanded view of 0.02s (indicated by red bar in Figure 1a) of the maximum variance component. (c) An expanded view of ∼.005s (indicated by red bar in Figure 1b). (d) Hodogram of maximum variance component vs. intermediate component for interval in Figure 1c. The projection of the geomagnetic field in the plane is plotted in black.

[3] The two-spacecraft STEREO mission [*Kaiser*, 2005] had four encounters with Earth's radiation belts during the orbit insertion phase. The Dec. 12, 2006 encounter provides a unique view of the Van Allen belts because it is the only time that two identically instrumented satellites have passed through this important region on near-identical orbital paths with a short (∼1.4 hour) delay, and because an explosive energy release process called a 'magnetospheric substorm' occurred between the times of the two passes. The STEREO S/WAVES instrument [*Bougeret et al.*, 2007] comprises three orthogonal 6m monopole antennas with electronics that provide frequency domain measurements of the electric field up to 16 MHz and waveform measurements using the Time Domain Sampler (TDS), which is designed to capture in high time resolution the largest amplitude waves. For this interval, the TDS sample length was 0.52s and the sample rate was 32 ksamples/s. The antenna response and effective boom lengths are discussed by *Bale et al.* [2007]. Effective boom lengths (and therefore wave amplitudes) are accurate to ∼ 25%. Because STEREO does not have a search-coil, Poynting flux measurements cannot be made.

2. STEREO Observations

[4] During the passage through the morning-side outer radiation belt, the TDS on STEREO-B, the second satellite to traverse the region, obtained twenty-four waveform samples, between ∼1120 and 1124 UT, with very large amplitude whistler-mode waves. Figure 1 shows an example of one sample with a peak electric field amplitude >200 mV/m, an order of magnitude larger than any previously reported in the radiation belts. Note that the largest amplitude occurs approximately in the center due to the TDS trigger algorithm. For the twenty-four samples, the observed maximum amplitudes ranged from ∼100 mV/m to ∼240 mV/m, but were occasionally larger as indicated by the saturation of the instrument during some samples. The whistler waves occurred in packets with a range of packet shapes and durations (on the order of ∼0.01 to .1 s). Based

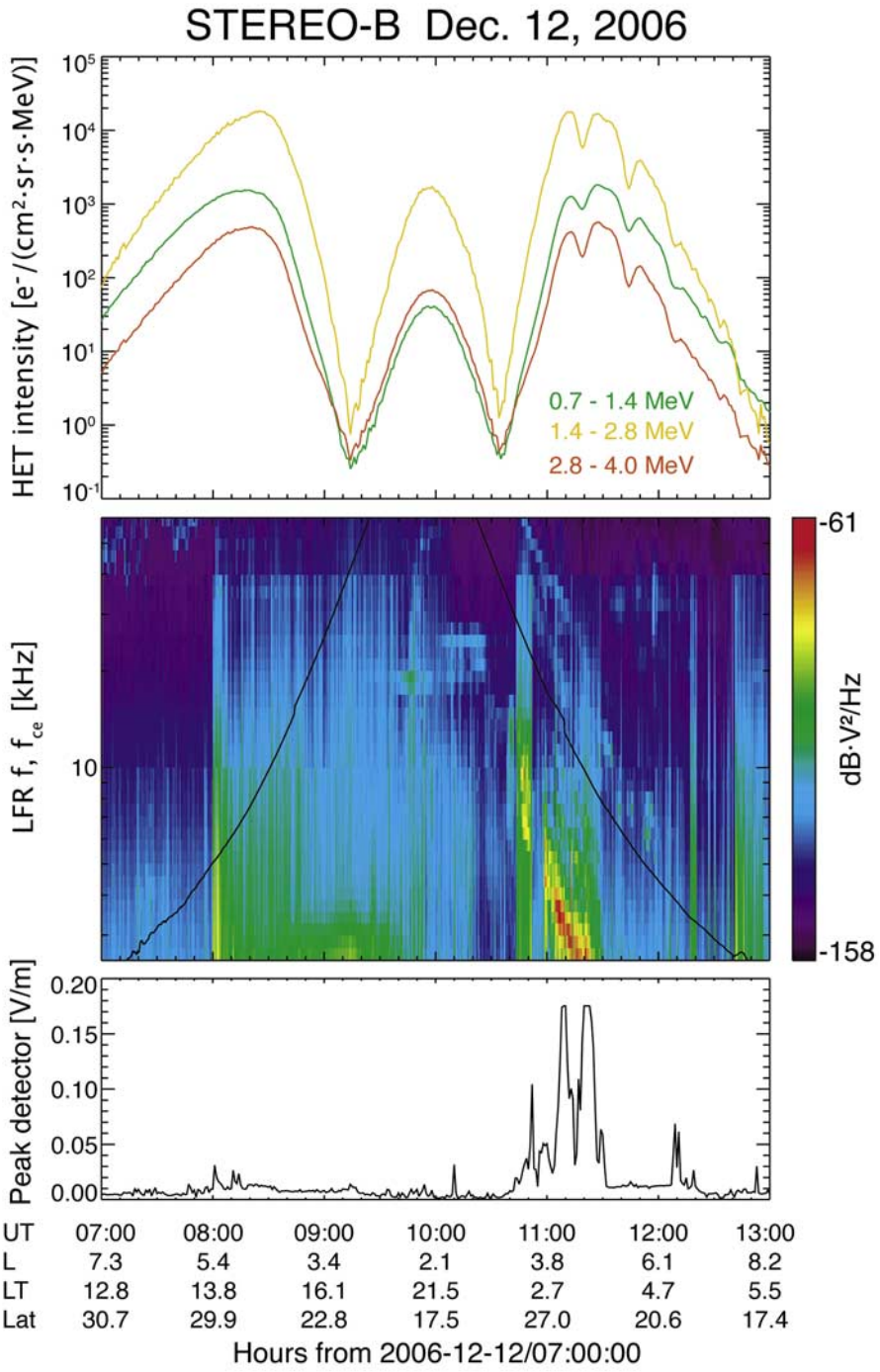

Figure 2. Overview of radiation belt observations on Dec. 12, 2006, obtained as STEREO-B moved from an L of 9 and LT (local time) ~12 to a perigee L = 2.1 and LT ~ 22 and back out to L = 6 and LT ~ 5. The 'L' value tags a geomagnetic field line by the radial distance in R_e at which the field line crosses the equatorial plane. (top) The intensity of electrons in three bands, 0.7–1.4 MeV, 1.4–2.8 MeV, and 2.8–4 MeV, from the IMPACT HET (High Energy Telescope) [*Luhmann et al.*, 2007; *von Rosenvinge et al.*, 2007]. Note that the amplitude modulation seen on the morning-side is due to spacecraft rotation. (middle) Plot of the power spectrum of the wave electric field from 2.5 kHz to 60 kHz. The black line indicates the value of f_{ce} calculated from the magnetic field measured by the IMPACT magnetometer. (bottom) The peak electric field in one dipole channel seen in each minute by the TDS peak detector (sampled at 125 kHz). Note that this peak detector saturated during several minutes in the region of interest.

on the average packet length, TDS sample duration and the latency in the TDS sampling, one can estimate that waves larger than ~100 mV/m occurred from ~1% to 4% of the time during the ~20 minute interval when large amplitude waves occurred (see discussion of Figure 2). For all the TDS samples, the frequency at peak power was ~0.2 f_{ce}, the electron cyclotron frequency, with multiple harmonics of the primary frequency. The electric field in the first harmonic was down by ~5–10 dB (a factor of ~2–5 in electric field) and the second harmonic was down by 20–25 dB. The hodogram (D) shows the effect of the multiple harmonics, as well as the propagation oblique to the geomagnetic field. The waves are right-hand polarized, consistent with the whistler mode.

[5] Figure 2 shows that the largest wave amplitudes during this event occurred within the inner (low L) region of the outer radiation belt on the morning-side. Due to data rate limitations, the TDS keeps in memory the largest amplitude wave events for transmission; thus, the regions where TDS samples are obtained are the regions with the largest amplitude waves. Although TDS samples were obtained only during the interval between ~11:20 and 11:24 UT, the electric field spectrum from the S/WAVES frequency domain instrument (Figure 2, middle) and peak detector data (Figure 2, bottom) indicate that the large amplitude whistler waves occurred from ~11:05–11:25 UT, with less intense whistlers from ~10:45–10:49 UT, covering the spatial region from L ~3.5 to 4.8, at magnetic latitudes ranging from ~21° to 26°, over local times from ~2 to ~3:45. The intense waves occurred during the recovery phase of a large substorm, as revealed by the AE index which reached a peak value of ~800 nT at ~10:50 UT, when a brief substorm injection of energetic electrons (~50–200 keV) was observed at geosynchronous orbit (6.6 R_e) by two Los Alamos National Laboratory satellites. It is generally accepted that, as these injected electrons drift dawnward due to magnetic field gradient and curvature drifts, they provide the energy source to drive whistler-mode waves. Although in this paper we do not address the source location, previous studies [*LeDocq et al.*, 1998; *Parrot et al.*, 2003] are consistent with a source region near the magnetic equatorial plane.

[6] Using the cold plasma dispersion relation [*Stix*, 1992], the phase velocity and magnetic field fluctuation amplitude, δB, for the waves can be estimated from the electric field in minimum variance coordinates. The waves are very oblique with the propagation angle with respect to the geomagnetic field ranging from ~45°–60°. Estimates of the phase velocity of ~35,000–70,000 km/s and δB~0.5–2 nT are obtained for a background plasma density of 2–5/cm^3 (estimated from the spacecraft potential, see *Pederson* [1995]) and measured geomagnetic field of 300–350 nT. The longitudinal electric field is the largest component, indicating that the waves were partly electrostatic, consistent with propagation near the resonance cone (resonance cone angle is ~77°). These results are also consistent with warm plasma dispersion calculations. Both the measurements and the warm dispersion results show that there is an electric field component parallel to the geomagnetic field on the order of 10% of the total field.

[7] In addition to the larger amplitudes, there are other distinctions between these observations and previously published studies of whistler-mode waves in the radiation belts. The lower band whistler 'chorus' waves (<0.5 f_{ce}) propagate parallel to the magnetic field (within ~10°) and are highly dispersive, usually with rising tones [*Goldstein and Tsurutani*, 1984; *Hayakawa et al.*, 1984]. In contrast, the waves described herein are monochromatic with frequency at peak power of ~0.2 f_{ce} throughout the 4 minute interval with waveform samples and the ~30 minutes when whistlers were seen in the spectrum. The waves were obliquely propagating and had a large longitudinal electric field component. Although the differences suggest that these very large amplitude whistlers may represent a new instability mechanism or free energy source, some differences may be due to propagation effects since whistlers propagating in an inhomogeneous medium can refract towards the resonance cone where the mode becomes quasi-electrostatic.

3. Discussion

[8] We have performed test particle simulations of electrons in a dipole-like magnetic field utilizing a code developed to look at electron interactions with a single constant amplitude, obliquely propagating whistler wave [*Roth et al.*, 1999]. The magnetic field gradient allows electrons to experience different gyroresonances as they move along the magnetic field, with a jump in energy and pitch angle associated with crossing each resonance. With the exception of wave amplitudes and propagation angles, which are based on the STEREO observations, the simulation parameters were identical to those of *Roth et al.* [1999]. The larger amplitude wave electric fields increase the electron trapping width in velocity space. In contrast to parallel-propagating whistlers, for which only the lowest order resonant interaction is effective, for obliquely propagating waves, higher order resonant interactions can occur, and more electrons can be resonant [*Kennel*, 1966]. Thus it is expected that observed waves can dramatically affect electrons and this is shown in preliminary results from the simulation. Electrons can gain ~0.1 to 4 MeV in the order of tens of ms. Scattering by angles of ~2° to 40° also occurs in similar times. These values are one to three orders of magnitude larger than those for the ~1 mV/m (or smaller) amplitudes typically assumed in radiation belt studies. Although the simulation assumes constant amplitude waves, the shorter duration of the observed wave packets may not affect the process because the interactions occur on such short times. Packets with peak amplitudes of 100 mV/m or larger were observed ~1–4% of the time for ~25 minutes, so electrons could encounter and resonate with many large amplitude packets during their bounce motion. The energy gains seen in the simulation are also consistent with those reported for a nonlinear acceleration mechanism associated with particle trapping that resulted in energy gains of ~0.5 MeV in ~1s for waves with amplitudes of tens of mV/m [*Omura et al.*, 2007]. The amplitudes required for the trapping are 1 to 2 orders of magnitude lower than seen in the STEREO data, while the energy gain in a single interaction scales as the wave amplitude. Thus, both simulation methods show that waves with the observed amplitudes can energize electrons by up to several MeV in short times (fractions of a second).

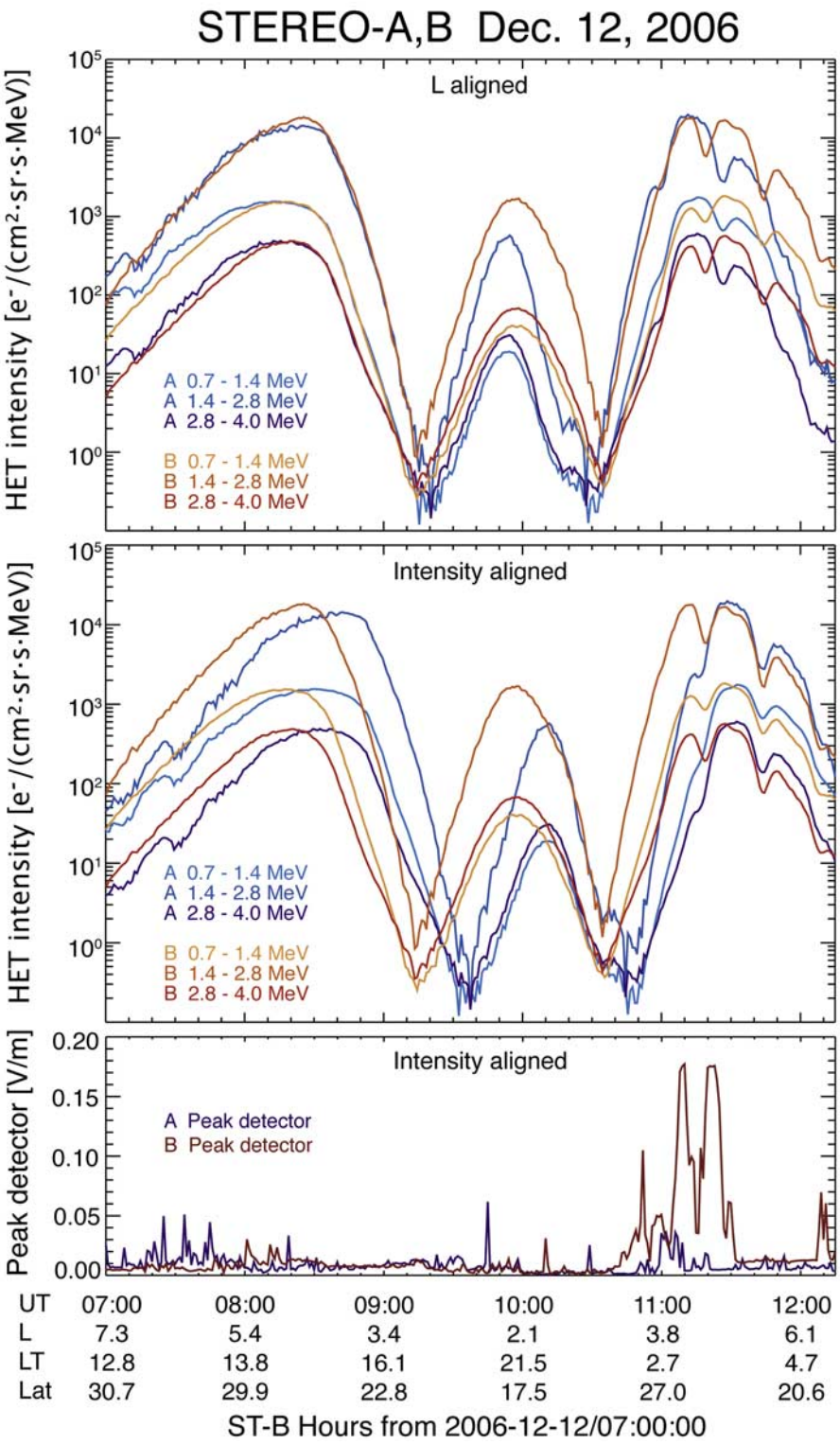

Figure 3. Comparison of the HET electron intensity on STEREO-A (red) and STEREO-B (blue) using two different methods for time lagging STEREO-A data. The time on the x-axis is the time at STEREO-B. (top) Plot of the data versus L-shell (1.4 hr lag for A). (middle) Line up of the maximum intensity for morning-side belt on the 2 satellites. (bottom) The TDS peak detector values for both satellites for the lag in Figure 3 (middle).

[9] STEREO-A led STEREO-B by ~1.4 hours in the radiation belt traversal, and the STEREO-A observations were obtained during a period of geomagnetic quiet. Figure 3 (top) shows that the MeV electron intensities seen by the two satellites were almost identical in the initial (afternoon) traversal of the outer belt, when the observations are plotted versus L-shell, demonstrating that the afternoon outer belt did not change during the ~1.4 hours between the

two encounters. The inner belt intensities were somewhat higher when observed by STEREO-B, but the peak location was only slightly changed. However, at the morning-side outer belt, the radiation belt has a broader extent in L and generally higher fluxes on STEREO-B (note that the minima are a result of the combined effect of instrument look angle, spacecraft rotation and electron anisotropy). Figure 3 (middle), in which the maximum intensity for the morning-side belt on the two satellites are aligned, suggests that there is a new region of enhanced MeV electron intensity at the low-L side of the radiation belt on STEREO-B. Both the L-alignment and the intensity alignment show clearly that the relativistic electrons were enhanced on STEREO-B. Because there was a substorm between the passage of STEREO-A and STEREO-B through the radiation belt, the geomagnetic field dipolarized and thus a given magnetic flux tube was closer to Earth during the passages of STEREO-B. This is consistent with the shift of $\sim$0.6 in L used in Figure 3 (middle). The peak detector values for both satellites are shown in Figure 3 (bottom) and indicate that no intense waves occurred during the STEREO-A encounter with the radiation belts. The differences seen by the two satellites are consistent with a picture in which the substorm-injected fresh electrons, with energies of $\sim$1–100 keV, excited large amplitude whistlers that energized electrons to produce the enhanced intensity of MeV electrons on a time-scale on the order of 10 minutes. The large amplitude, obliquely propagating waves resulted in energization on time-scales much shorter than the $\sim$1 day expected from most current radiation belt models that utilize a quasi-linear approach to whistler interactions [*Horne et al.*, 2003]. As noted above, the simulations showed large pitch angle changes, in addition to rapid energization. Corroborating evidence of rapid (<1s) scattering is provided by observations of short-time scale variations in loss rates ('microbursts') of MeV electrons by SAMPEX simultaneous with the STEREO observations [*Blake et al.*, 1996; *Millan and Thorne*, 2007; J. B. Blake, private communication, 2007].

[10] The measurements of large amplitude waves and enhanced intensity of electrons occurred within a solar wind high-speed stream. The solar wind conditions were relatively constant throughout the day, as observed by ACE, with speeds of $\sim$650–700 km/s and density of $\sim$2/cm^3, typical of a high-speed stream. Thus, the STEREO observations are consistent with studies correlating enhanced fluxes with high speed streams [*Paulikas and Blake*, 1979]. Although the observations occurred after a substorm injection, it was a weak and short-lived injection compared to those typically observed. In addition, these waves did not occur during a magnetic storm. Given the much more dramatic changes in the radiation belts seen during storms and that much larger substorm injections are observed, it is likely that waves of comparable amplitude are not unusual and that even larger amplitude whistler waves may occur. The discovery of these waves was enabled by the STEREO TDS instrument, which makes time domain measurements of the full 3d electric field with a very large dynamic range and which is designed to capture the largest amplitude waves. These new observations suggest that the standard quasi-linear approach to studies of energization and scattering may not be adequate to understand radiation belt dynamics because the large amplitude waves generate nonlinear effects, including trapping, resulting in energization or scattering loss in one wave packet encounter.

[11] **Acknowledgments.** We thank J. Dombeck and P. Schroeder for programming assistance and B. Lavraud for providing LANL data. ACE plasma data, courtesy D. J. McComas, and magnetic field data, courtesy N. Ness, were obtained from CDAWEB, and AE, from WDC for Geomagnetism, Kyoto. This work was supported by NASA through the Solar Terrestrial Probes and Living With A Star programs. Test particle simulations were performed at the University of Minnesota Supercomputing Institute for Digital Simulation and Advanced Computation.

References

Albert, J. M., and S. L. Young (2005), Multidimensional quasi-linear diffusion of radiation belt electrons, *Geophys. Res. Lett.*, *32*, L14110, doi:10.1029/2005GL023191.

Bale, S. D., et al. (2007), The electric antennas for the STEREO/WAVES experiment, *Space Sci. Rev.*, in press.

Blake, J. B., et al. (1996), New high temporal and spatial measurements by SAMPEX of the precipitation of relativistic electrons, *Adv. Space Res.*, *18*(8), 171.

Bougeret, J. L., et al. (2007), S/Waves: The radio and plasma wave investigation on the STEREO Mission, *Space Sci. Rev.*, in press.

Friedel, R. H., G. D. Reeves, and T. Obara (2002), Relativistic electron dynamics in the inner magnetosphere: A review, *J. Atmos. Sol. Terr. Phys.*, *64*, 265.

Goldstein, B. E., and B. T. Tsurutani (1984), Wave normal directions of chorus near the equatorial source region, *J. Geophys. Res.*, *89*, 2789.

Gurnett, D. A., R. L. Huff, and D. L. Kirchner (1997), The wide-band plasma wave investigation, *Space. Sci. Rev.*, *79*, 195.

Gustaffson, G., et al. (1997), The spherical probe electric field and wave experiment, *Space. Sci. Rev.*, *79*, 31.

Hayakawa, M., Y. Yamanaka, M. Parrot, and F. Lefeuvre (1984), The wave normals of magnetospheric chorus emissions observed on board GEOS 2, *J. Geophys. Res.*, *89*, 2811.

Horne, R. B., and R. M. Thorne (2003), Relativistic electron acceleration and precipitation during resonant interactions with whistler-mode chorus, *Geophys. Res. Lett.*, *30*(10), 1527, doi:10.1029/2003GL016973.

Horne, R. B., S. A. Glauert, and R. M. Thorne (2003), Resonant diffusion of radiation belt electrons by whistler-mode chorus, *Geophys. Res. Lett.*, *30*(9), 1493, doi:10.1029/2003GL016963.

Horne, R. B., R. M. Thorne, S. A. Glauert, J. M. Albert, N. P. Meredith, and R. R. Anderson (2005), Timescale for radiation belt electron acceleration by whistler mode chorus waves, *J. Geophys. Res.*, *110*, A03225, doi:10.1029/2004JA010811.

Hudson, M., et al. (2007), Relationship of the Van Allen radiation belts to solar wind drivers, *J. Atmos. Sol. Terr. Phys*, in press.

Kaiser, M. L. (2005), The STEREO mission, *Adv. Space Res.*, *36*(8), 1483.

Kennel, C. F. (1966), Low frequency whistler mode, *Phys. Fluids*, *9*, 2190.

Kennel, C. F., and H. E. Petschek (1966), Limit on stably trapped particle fluxes, *J. Geophys. Res.*, *71*, 1.

LeDocq, M., D. A. Gurnett, and G. B. Hospadarsky (1998), Chorus source location from VLF Poynting flux measurements with the Polar spacecraft, *Geophys. Res. Lett.*, *25*, 4063.

Luhmann, J., et al. (2007), STEREO IMPACT investigation goals, measurements, and observations overview, *Space Sci. Rev.*, in press.

Meredith, N. P., R. B. Horne, and R. R. Anderson (2001), Substorm dependence of chorus amplitudes: Implications for the acceleration of electrons to relativistic energies, *J. Geophys. Res.*, *106*, 13,165.

Millan, R., and R. M. Thorne (2007), Review of radiation belt relativistic electron losses, *J. Atmos. Sol. Terr. Phys.*, *69*, 362.

Omura, Y., N. Furuya, and D. Summers (2007), Relativistic turning acceleration of resonant electrons by coherent whistler-mode waves in a dipole magnetic field, *J. Geophys. Res.*, *112*, A06236, doi:10.1029/2006JA012243.

Parrot, M., et al. (2003), Source locations of chorus observed by Cluster, *Ann. Geophys.*, *21*, 473.

Paulikas, G. A., and J. B. Blake (1979), Effects of the solar wind on magnetospheric dynamics: Energetic electrons at the synchronous orbit, in *Quantitative Modeling of Magnetospheric Processes*, *Geophys. Monogr. Ser.*, vol. 21, edited by W. P. Olson, p. 180, AGU, Washington, D. C.

Pederson, A. (1995), Solar wind and magnetospheric plasma diagnostics by spacecraft electrostatic potential measurements, *Ann. Geophys.*, *13*, 118.

Roth, I., M. Temerin, and M. K. Hudson (1999), Resonant enhancement of relativistic electrons during geomagnetically active periods, *Ann. Geophys.*, *17*, 631.

Santolík, O., D. A. Gurnett, J. S. Pickett, M. Parrot, and N. Cornilleau-Wehrlin (2003), Spatio-temporal structure of storm-time chorus, *J. Geophys. Res.*, *108*(A7), 1278, doi:10.1029/2002JA009791.

Schulz, M., and L. J. Lanzerotti (1974), *Particle Diffusion in the Radiation Belts*, Springer, New York.

Stix, T. H. (1992), *Waves in Plasmas*, Am. Inst. of Phys., New York.

Summers, D., and C.-Y. Ma (2000), A model for generating relativistic electrons in the Earth's inner magnetosphere based on gyroresonant wave-particle interactions, *J. Geophys. Res.*, *105*, 2625.

Summers, D., R. M. Thorne, and F. Xiao (1998), Relativistic theory of wave-particle resonant diffusion with application to electron acceleration in the magnetosphere, *J. Geophys. Res.*, *103*, 20,487.

von Rosenvinge, T. T., et al.(2007), The high energy telescopes for STEREO, *Space Sci. Rev.*, in press.

M. Acuna and T. von Rosenvinge, NASA Goddard Space Flight Center, Mail Code 696, Greenbelt, MD 20771, USA.

S. D. Bale, I. Roth, and M. Temerin, Space Sciences Laboratory, University of California, Berkeley, 7 Gauss Way, Berkeley, CA 94720-7450, USA.

C. Cattell, K. Goetz, P. J. Kellogg, K. Kersten, and J. R. Wygant, School of Physics and Astronomy, University of Minnesota, 116 Church Street SE, Minneapolis, MN 55455, USA. (cattell@fields.space.umn.edu)

R. Ergun, Laboratory for Atmospheric and Space Physics, University of Colorado, Campus Box 530, Boulder, CO 80303, USA.

M. K. Hudson, Department of Physics, Dartmouth College, Box 6127, Hanover, NH 03755, USA.

M. Maksimovic, Laboratoire d'Etudes Spatiales et d'Instrumentation en Astrophysique, Observatoire de Paris, 5 Place J. Janssen, F-92195 Meudon, France.

R. A. Mewaldt, Downs Laboratory, California Institute of Technology, Pasadena, CA 91125, USA.

C. T. Russell, Institute for Geophysics and Planetary Physics, University of California, Los Angeles, 405 Hilgard Avenue, Los Angeles, CA 90095-1567, USA.

M. Wiedenbeck, Jet Propulsion Laboratory, California Institute of Technology, 4800 Oak Grove Drive, Pasadena, CA 91109, USA.